Modeling a neuronal network as coupled spin–boson systems and seizure as a fluorescence- to superradiance-like phase transition

Hugo Sanchez and Miled H. Y. Moussa

Instituto de Física de São Carlos, Universidade de São Paulo, Av. Trab. São Carlense 400, São Carlos, 13560-970, Brasil

Corresponding author. E-mail: hugo.sanchezdearaujo@gmail.com

Abstract

Since the pioneering work of Onuchic, Beratan, and Hopfield (OBH) [Onuchic, J. N. et al. The Journal of Physical Chemistry, v. 90, n. 16, p. 3707-3721, 1986.], it has been well established that electron transfer in chemical reactions can be modeled by the decaying probability of excitation dynamics in the spin–boson system. In analogy to the OBH framework, we propose a model wherein electric current generation in a neuron is equally described through population inversion in a spin–boson system. Building on this connection, we extend our approach to model the collective firing activity characteristic of seizures by representing the neuronal network as a set of coupled spin–boson units. We demonstrate that under specific circumstances our model releases electric current in a comb of superpulses which bears similarity with the phenomenon of superradiant radiation emission in atomic optics. Our model seems to be in perfect agreement with the multiple synchronized firings observed in a convulsive seizure. With the normal current transfer regime being the analog to the fluorescence emission in atomic optics, we thus model seizure as a fluorescence- to superradiance-like phase transition. Furthermore, our model also provides us an understanding of the mechanism by which we can disarm seizure, protecting the brain from sequelae resulting from the ictal stage of the process. We finally observe that from the input of experimentally measured and theoretically estimated parameters, our model is able to deliver reasonable results, in accordance with the neuroscience literature, for the rate of energy produced by a neuron in the normal current transfer regime, the energy released per neuron in a 1 minute seizure and the time interval for a single comb of supercurrents.

1 Introduction

Understanding the complex behavior of neuronal dynamics has become one of the most important topics in modern neuroscience and biophysics since it is directly connected with neuronal disorders [2-5]. The brain is responsible for controlling multiple processes such as emotions, vision, motor skills, breathing, and memory [6-10]. The main structure that makes possible this accurate level of control is the neuronal network [11], capable of sending and receiving electrical stimuli along the whole body, where different signals are interpreted as a specific sensation or command.

Based on the intensity of received electrical stimulation, a neuron can either become excited and generate a firing response or remain at rest [12,13]. When the stimulus is sufficiently strong, reaching an electrical potential threshold of approximately -55 mV, the neuron's cell membrane depolarizes due to an influx of sodium ions, generating a signal known as action potential [14]. Information is propagated within the neuronal network through electrical synapses, which are gap junctions allowing direct communication, and chemical synapses, involving the release of neurotransmitters [15,16]. These synapses can result in excitatory or inhibitory responses in postsynaptic neurons [17]. The balance between excitation and inhibition is crucial for normal brain function [18]. However, when this balance is disrupted and excitation prevails over inhibition, neurons may begin to fire synchronously, leading to partial or generalized seizures, involving a specific or total area of the brain, respectively [19-21].

The precise mechanism underlying seizures involves a complex interplay of various molecular and cellular changes that are not completely understood [22-25]. However, the main factors contributing to seizures include pyramidal neurons activity [26,27], astrocytes [28,29], interneurons [30], alterations in synaptic connections, gap junctions [31,32], and extracellular ion concentrations [33]. These factors are directly connected with the development of seizures [34-36]. Intense excitatory activity in pyramidal neurons triggers an abnormal

depolarizing phase known as the paroxysmal depolarizing shift [37-40]. This phenomenon primarily arises from the activation of glutamate-mediated receptors, specifically AMPA and NMDA receptors [41,42], in conjunction with voltage-gated calcium channels [43,44]. The intense firing of action potentials leads to a reduction in inhibitory synaptic transmission mediated by GABAergic interneurons [45-48]. Additionally, chronic changes in dendritic structure [49,50], receptor density [51], and extracellular potassium ion levels [52] also contribute to the loss of surround inhibition, which may lead to the synchronous firing process observed during seizures. Neurodegenerative disorders such as Alzheimer's, Parkinson's, and Huntington's disease can sometimes be accompanied by seizures [53-57]. They are characterized by the progressive degeneration and loss of nerve cells in the brain, leading to a wide range of cognitive, motor, and behavioral symptoms.

In the past decade, numerous experiments have been conducted for a deeper understanding of crucial mechanisms that are activated during seizures. These investigations have focused on various aspects, including the role of the brain glucose transporter [58,59], the changes in the serum blood-brain barrier following tonic-clonic seizures [60-62], the signaling pathways involving the NLRP3 regulator [63-65], and the alterations in bioenergetics [66-68]. These findings have provided evidence that disruptions in cellular or mitochondrial metabolism can serve as primary factors in the initiation of seizures and the subsequent development of spontaneous recurrent seizures. Such discoveries hold immense potential in advancing the development of therapeutic interventions for pharmacoresistant epilepsy and neurodegenerative disorders.

In the early 1960s, physicists proposed that quantum effects were present in biological systems. During this period, Löwdin [69] presented the first quantum biological model to explain the occurrence of spontaneous tautomeric mutations in DNA molecules through the proton tunneling mechanism. Since then, quantum mechanics has proven to be essential for understanding several topics in biology such as quantum effects in bacterial photosynthetic

energy transfer [70,71], photosynthesis [72,73], electron transfer in proteins [74,75], quantum biology of retinal [76] and vibrationally assisted transport in transmembrane proteins [77]. Moreover, a model for tautomeric mutations in DNA based on the amplificative-dissipative tunneling mechanism has recently been presented in Ref. [78].

Many contributions have been devoted for developing mathematical and computational models for seizure dynamics [79-82]. In Ref. [82], invariant properties are identified to characterize seizures under different physiological and pathological conditions. An explanation for different features of seizure onset patterns using the bifurcation analyses of a dynamical brain model is given in Ref. [79]. In Ref. [81], a computational model is considered to characterize focal or generalized seizure based on the pattern of connection in brain networks. We finally mention a mathematical model constructed to analyze how interrelated dynamics of sodium and potassium affects the occurrence of seizure [80].

In 1996, Penrose and Hameroff [83] proposed the hypothesis that microtubules present in neurons could exhibit quantum behavior in a state of superposition. Despite this proposal, no observations confirming the existence of quantum coherence in brain microtubules were obtained. Thus, the idea of quantum effects in the brain had not been widely accepted and remained an open topic of investigation. However, recent experimental evidence presented by Kerskens and Pérez [84], who collected signals through nuclear magnetic resonance, may indicate entanglement mediated by consciousness-related brain functions.

Here, we approach seizure by modeling the neuronal generation of electric current in analogy to the Onuchic, Beratan and Hopfield (OBH) [1] treatment for the electron transfer in chemical reactions. In the OBH model it is demonstrated that under reasonable approximations, the complex mechanism of electron transfer between two trapped sites, the electron donor and acceptor, is approximated by the decaying probability of the excitation dynamics in the spin–boson model [85]. Reasoning by analogy with Ref. [1], it seems reasonable to conjecture that the electric current generation along the axon of a neuron may also be de-

scribed by the population inversion in a spin–boson system. While we cannot assume that the OBH model can be directly applied to describe electric current generation in neurons, which primarily use ion flow instead of electron transfer to fire action potentials, its theoretical constructs could inspire analogous modeling in neurobiological contexts. In favor of our conjecture is the argument that a neuron presents unambiguously the rest and firing states –the absence or presence of electric current– which we associate with the donor and acceptor states in the OBH model. Furthermore, through this approach we have in advance the parameters given in the neuroscience literature for the well-known bias transition energy between the rest and firing states of the spin–boson system, as well as the energy associated with synaptic transmissions, which provides the coupling frequency between neurons.

It could be argued that the macroscopic dimension of the neuron would invalidate the quantum tunneling process associated with the spin–boson model. On this regard, we observe that a spin–boson model adopted to describe the generation of current in the neuron can be linked to the non-local tunneling process described in Ref. [86]. In this non-local tunneling there is no direct overlap of the wave functions in the energy wells associated with the rest and firing states. The rest state represents the electrons trapped in the negative ions within the soma (cellular body), while the firing state represents the electrons after tunneling to the dendrites. These rest and firing wells can be distant from each other, connected by a chain of quantum systems, which in the neuron would be the voltage-gated ion channels. The overlap between the wave functions of the rest and firing states occurs indirectly through the wave function of the entire chain of voltage-gated channels. In this case, the tunneling of electrons between the rest and firing states will occur in such a way that these electrons should only virtually populate the myelin sheaths between the voltage-gated channels. This virtual occupation of the myelin sheaths makes non-local tunneling a high-probability process, practically free from the dissipation effects of the environment. Here, it is important to emphasize two points: (i) the spin–boson model based on the non-local tunneling can effectively be described by the local tunneling as illustrated in Fig. 1; (ii) the demonstration

of our conjecture that the firing process in a neuron can be described by the spin–boson model is by itself a most interesting and challenging work.

Under our conjecture, the neuronal network is then modeled as coupled spin–boson systems, and we then demonstrate that the synchronous firing characterizing seizures, the rapid oscillations in electroencephalogram (EEG), is a comb of superradiant-like current pulses. The Dicke [87] superradiance predicted in 1954, is a collective effect that occurs when a moderately dense sample of N atoms with decay rate γ interacts with both its environment and the electromagnetic radiation it emits. Instead of emitting independently and randomly, in a fluorescence pulse of duration and intensity proportional to $1/\gamma$ and N, the atoms synchronize their emissions to release energy in a highly coherent pulse of duration and intensity proportional to $1/N\gamma$ and N^2. Analogously, it follows from our network that a synchronized emission of multiple supercurrent pulses is generated when the neurons are strongly coupled to each other, corroborating that the intensity of this comb of pulses is a distinctive feature of seizures. Remarkably, this entire comb of supercurrents is enveloped within the typical emission time $1/N\gamma$ of a single Dicke superradiant pulse, the time width of each of our supercurrent being around $1/N^u\gamma$, and their intensities reaching N^v, with real $u, v > 1$. The comb of supercurrents emerging from our model seems to reasonable explain the multiple synchronized firings observed in seizures with the normal neuronal activity being described in analogy to the fluorescence emission in atomic physics.

Therefore, the distinctive features of our model lies in the characterization of seizures as a fluorescent- to superradiance-like phase transition; with the time width of each pulse that make up the supercurrent comb, around $1/N^u\gamma$, being a unique phenomenon in many-body physics.

Although the classical framework introduced by Hodgkin and Huxley remains a cornerstone for modeling the electrical excitability of individual neurons through voltage-gated ionic currents, it does not, in its original form, account for the emergence of synchronized

activity across neuronal populations. To overcome this limitation, researchers have developed extended models that embed the Hodgkin–Huxley equations within neural networks, incorporating synaptic interactions, extracellular ion dynamics, and modulatory biochemical pathways. For example, Bazhenov et al. [88] simulated thalamocortical oscillations linked to absence epilepsy using a network of coupled neurons; Fröhlich and Bazhenov [89] examined how changes in synaptic strength can drive transitions between normal and pathological brain states. Although our model does not explicitly accounts for the ionic conductance dynamics described by the Hodgkin and Huxley equations, it captures the fundamental process of neuronal excitation —the sodium influx in Hodgkin–Huxley model— through the transition between rest and firing states, with the resulting supercurrents reflecting the propagation of action potentials. Rather than modeling the electrophysiological mechanisms, our approach retains a microscopic analysis emphasizing collective neuronal synchronization.

2 The model

Based on the discussion in the Introduction, we then model our neuronal network by the Hamiltonian ($\hbar = 1$)

$$\begin{aligned}\mathcal{H} = &\sum_{m=1}^{N}\left[\frac{1}{2}\left(\omega_0\sigma_z^m + \Delta\sigma_x^m\right) - g\sum_{n(\neq m)=1}^{N}\left(\sigma_+^m\sigma_-^n + \sigma_-^m\sigma_+^n\right)\right] \\ &+ \sum_{m=1}^{N}\sum_{\ell=1}^{\infty}\left(\frac{\left(P_\ell^m\right)^2}{2M_\ell^m} + \frac{1}{2}M_\ell^m\left(\omega_\ell^m\right)^2\left(R_\ell^m\right)^2\right) + \sum_{k=1}^{\infty}\left(\frac{P_k^2}{2M_k} + \frac{1}{2}M_k\omega_k^2R_k^2\right) \\ &+ \sum_{m=1}^{N}\left(\sigma_+^m + \sigma_-^m\right)\left(\sum_{\ell=1}^{\infty}\lambda_\ell^m R_\ell^m - \sum_{k=1}^{\infty}\lambda_k R_k\right), \end{aligned} \tag{1}$$

where the first term describes the set of N neurons as asymmetric double–well potentials, with σ_z, σ_x and $\sigma_\pm$ being Pauli spin operators. As shown in Fig. 1, $\hbar\omega_0$ is a positive bias energy between the lower and upper wells corresponding to the rest and firing eigenstates $|\downarrow\rangle$

and $|\uparrow\rangle$ of σ_z. Δ is a tunneling frequency associated with the spontaneous neuronal activity. The second term models the interconnection between the neurons, where g is the coupling between pre– and post–synaptic excitatory ($g \neq 0$) and inhibitory ($g = 0$) neurons, related to glutamate and GABAergic neuronal responses respectively. We consider a symmetric network where all the neurons interact with each other based on the knowledge that a neuron has thousands of synaptic connection with the others. Moreover, this symmetric network makes it simpler to approach the problem via mean–field and Holstein–Primakoff transformations.

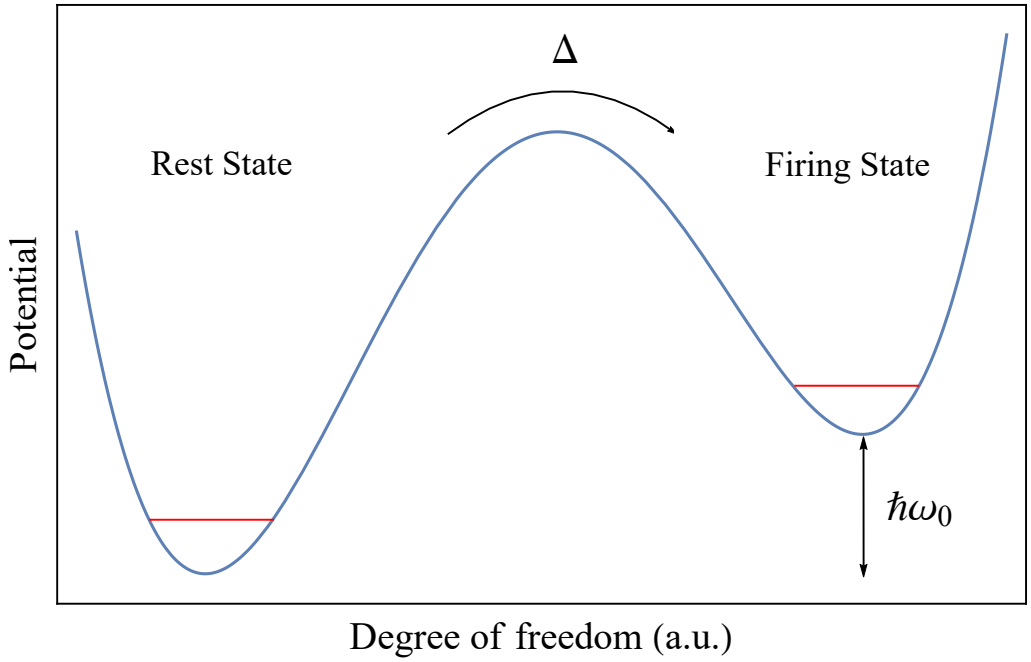

Figure 1: Modeling a neuron as a spin–boson system with two unbiased rest and firing states, connected by the tunneling rate Δ.

We assume that each neuron is coupled to its own reservoir, with strength λ_ℓ^m, as described by the fifth term of the Hamiltonian. The reservoirs, representing the cerebrospinal fluid, are described by the third term as a collection of independent harmonic oscillators with frequencies ω_ℓ^m, masses M_ℓ^m, positions R_ℓ^m, and momenta P_ℓ^m. We have also considered an anti-reservoir, given by the fourth term of the Hamiltonian, to describe either an internal

or external multimodal amplification source, or even both simultaneously, which, as we show, is able to disarm the seizure mechanism. This possibility, by means of an external multimodal source, has been suggested in Refs. [90,91]. Here, we observe that the neuronal network itself, with the exception of the epileptic focus, may also act to suppress seizure as an internal amplification source associated with the residual excitation of the network. The amplification character of the anti-reservoir follows from the negative sign of its coupling λ_k with the network, as given by the sixth term of the Hamiltonian.

In order to derive a master equation for our system, we first diagonalize the network represented by the second term in the Hamiltonian (1) using the collective Holstein–Primakoff [92] transformations, a mapping from spin operators to boson creation and annihilation operators, given by

$$S_+ = \sqrt{N - A^\dagger A}\, A \simeq \sqrt{N}\, A, \tag{2a}$$

$$S_- = A^\dagger \sqrt{N - A^\dagger A} \simeq \sqrt{N}\, A^\dagger, \tag{2b}$$

$$S_z = \frac{N}{2} - A^\dagger A, \tag{2c}$$

where the approximations in $(2a)$ and $(2b)$ are valid in the limit $N \gg \left\langle A^\dagger A \right\rangle$, with $S_z = \sum_m \sigma_z^m/2$ and $S_\pm = \sum_m \sigma_\pm^m$. Inserting Eqs. $(2a)$, $(2b)$ and $(2c)$ in (1), we get

$$\tilde{\mathcal{H}} = \Omega A^{\dagger}A + \Delta\sqrt{N}\left(A + A^{\dagger}\right) + \sum_{m,\ell}\left(\frac{(P_{\ell}^{m})^{2}}{2M_{\ell}^{m}} + \frac{1}{2}M_{\ell}^{m}\left(\omega_{\ell}^{m}\right)^{2}\left(R_{\ell}^{m}\right)^{2}\right) + \sum_{k}\left(\frac{P_{k}^{2}}{2M_{k}} + \frac{1}{2}M_{k}\omega_{k}^{2}R_{k}^{2}\right) + \sqrt{N}\left(A + A^{\dagger}\right)\left(\sum_{m=1}^{N}\sum_{\ell=1}^{\infty}\lambda_{\ell}^{m}R_{\ell}^{m} - \sum_{k=1}^{\infty}\lambda_{k}R_{k}\right), \tag{3}$$

where we neglected constant terms and corrections of order $\mathcal{O}(1/N)$ in the limit of large N. From Eq. (3), we derive the master equation for the collective bosonic mode given by

$$\dot{\rho}_{N}(t) = -i\left[\tilde{H}_{\mathcal{S}}, \rho_{N}\right] - i\,\mathscr{J}(\Omega)\left[X, \{P, \rho_{N}\}\right] - \mathscr{J}(\Omega)\,coth\left(\frac{\Omega}{k_{B}T}\right)\left[X, [X, \rho_{N}]\right], \tag{4}$$

where $\tilde{H}_{\mathcal{S}} = \Omega A^{\dagger}A + \Delta\sqrt{N}\left(A + A^{\dagger}\right)$, $\mathscr{J}(\Omega) = \sum_{m} J_{1}^{m}(\Omega) - J_{2}(\Omega)$, with $J_{1}^{m}(\omega)$ and $J_{2}(\omega)$ representing the spectral density of the m-th reservoir and of the anti-reservoir, respectively, while $X = \left(A + A^{\dagger}\right)$ and $P = -i\left(A - A^{\dagger}\right)$. Assuming Ohmic spectral densities for both the counter-acting baths, such that $J(\omega) = \eta\omega$, where $\eta = \gamma/2\omega_{0}$, γ being an effective relaxation rate [93], it follows that $\mathscr{J}(\omega) = \left(\sum_{m}\eta_{1}^{m} - \eta_{2}\right)\omega$. Switching back to the spin representation, after diagonalizing the Hamiltonian (1), we rewrite the master equation for the reduced density operator of the neuronal network as

$$\dot{\rho}_{N}(t) = -\imath\left[\mathcal{H}_{\mathcal{S}}, \rho_{N}\right] + \sum_{m}\left(\mathcal{L}_{m}\rho_{N} + \sum_{n}\mathcal{L}_{mn}\rho_{N}\right), \tag{5}$$

where $\mathcal{H}_{\mathcal{S}} = \sum_{m}\left(\Omega\sigma_{z}^{m} + \Delta\sigma_{x}^{m}\right)/2$, noting that the couplings between neurons was absorbed by the effective frequency $\Omega = \omega_{0} + 2Ng$. The diagonal dissipative channels, describing the energy decay of each neuron, are given by

$$\mathcal{L}_m\rho_N = \frac{\mathscr{J}(\omega_0)}{N}\left(\left[\sigma_+^m, \rho_N\sigma_-^m\right] - \left[\sigma_-^m, \sigma_+^m\rho_N\right] - \left[\sigma_+^m, \sigma_+^m\rho_N\right] + \left[\sigma_-^m, \rho_N\sigma_-^m\right]\right), \tag{6}$$

while the non-diagonal channels, resulting from the coupling between neurons, obey

$$\mathcal{L}_{mn}\rho_N = \frac{\left(\mathscr{J}(\Omega) - \mathscr{J}(\omega_0)\right)}{N}\left(\left[\sigma_+^m, \rho_N\sigma_-^n\right] - \left[\sigma_-^m, \sigma_+^n\rho_N\right] - \left[\sigma_+^m, \sigma_+^n\rho_N\right] + \left[\sigma_-^m, \rho_N\sigma_-^n\right]\right). \tag{7}$$

Regarding Eq. (5), we first observe (i) that the non-diagonal channels are evidently suppressed for $g = 0$, once $\Omega = \omega_0$. In this case, the master equation reduces to the expected form for N independent dissipative neurons. (ii) In the regime of strong coupling between the neurons, $2Ng \gtrsim \omega_0$, when the non-diagonal channels are strengthened, all the independent reservoirs act as a single one for all the network, such that

$$\sum_{m,n}\mathcal{L}_{mn}\rho_N = \Gamma\left([S_+, \rho_N S_-] - [S_-, S_+\rho_N] - [S_+, S_+\rho_N] + [S_-, \rho_N S_-]\right), \tag{8}$$

where $\Gamma = 2g\left(\sum_m \eta_1^m - \eta_2\right)$, which simplifies to $\Gamma = (Ng/\omega_0)\,\gamma - 2g\eta_2$ when considering, from here on, the same damping constant for all the reservoirs: $\eta_1^m = \eta$. In this regime, the master equation leads to emergent collective effects analogously to the Dicke superradiance where, as anticipated above, a moderately dense atomic sample interacts with a single reservoir. We can draw a parallel between our model and Dicke's superradiance by associating each atom in the moderately dense sample with a spin–boson unit in a network in which they are strongly coupled. (iii) We finally stress that the non-diagonal channels can be weakened when the spectral density function of the anti-reservoir emulates that of the reservoirs, with $\eta_2 = \alpha N\eta$ and $0 \leq \alpha \leq 1$. Under this condition, $\Gamma = (1-\alpha)\,(Ng/\omega_0)\,\gamma$, with the suppression of the non-diagonal channel for $\alpha = 1$. The observations (i)–(iii) are in agreement with Ref. [94],

where a general treatment is given for a network of coupled dissipative systems.

Next, under the assumption of the strong coupling regime, we approach Eqs. (5) and (8) through the mean-field approximation [95], tracing out the degrees of freedom of $N-p$ neurons, such that $\sum_{i=p+1}^{N} T_{rp+1,\ldots,N}\sigma_{\pm}^{i}\rho_N = (N-p)\, T_{rp+1,\ldots,N}\sigma_{\pm}^{i}\rho_N$ for $i > p$. We are left with a remaining network of p strongly-coupled neurons under the action of a common reservoir, described by

$$\begin{aligned}\dot{\rho}_p(t) = &-\frac{i}{2}\sum_{m=1}^{p}\left[\Omega\sigma_z^m + \Delta\sigma_x^m, \rho_p\right] \\ &+ \Gamma\sum_{m,n}\left(\left[\sigma_+^m, \rho_p\sigma_-^n\right] - \left[\sigma_-^m, \sigma_+^n\rho_p\right] - \left[\sigma_+^m, \sigma_+^n\rho_p\right] + \left[\sigma_-^m, \rho_p\sigma_-^n\right]\right) \\ &+ \Gamma(N-p)\sum_{m}\Big(\left[\sigma_+^m, Tr_{p+1}\sigma_-^{p+1}\rho_{p+1}\right] - \left[\sigma_-^m, Tr_{p+1}\rho_{p+1}\,\sigma_+^{p+1}\right] \\ &- \left[\sigma_+^m, Tr_{p+1}\rho_{p+1}\,\sigma_+^{p+1}\right] + \left[\sigma_-^m, Tr_{p+1}\sigma_-^{p+1}\rho_{p+1}\right]\Big). \end{aligned} \tag{9}$$

For $p = 1$, and assuming $\rho_2 = \rho_1^1 \otimes \rho_1^2$, the one–body master equation becomes

$$\dot{\rho}_1(t) = -i\left[\mathcal{H}_{SR}, \rho_1\right] + \Gamma\left\{[\sigma_+, \rho_1\sigma_-] - [\sigma_-, \sigma_+\rho_1] - [\sigma_+, \sigma_+\rho_1] + [\sigma_-, \rho_1\sigma_-]\right\}, \tag{10}$$

where

$$\mathcal{H}_{SR} = \frac{\Omega}{2}\sigma_z + \frac{\Delta}{2}\sigma_x + \Gamma(N-1)\langle\sigma_y\rangle\,\sigma_x, \tag{11}$$

is a nonlinear mean-field Hamiltonian. The Von Neumann term of Eq. (10) describes the dynamics of the network representative neuron while the remaining terms, related with dissipative effects coming only from the non-diagonal channels, can be neglected for collective processes that occur in a time interval much shorter than Γ^{-1}. The mean field approximation then applies only to short-time phenomena, and in this case, the master equation (10)

reduces to a nonlinear Schrödinger equation for the Hamiltonian $\mathcal{H}_{SR}$. It can be solved through the Lewis and Riesenfeld [96] method, by proposing the dynamical invariant $I(t) = \langle\sigma_x\rangle\,\sigma_x + \langle\sigma_y\rangle\,\sigma_y + \langle\sigma_z\rangle\,\sigma_z$ satisfying

$$\frac{dI}{dt} = \frac{\partial I}{\partial t} - \imath\,[I, H_{SR}] = 0. \tag{12}$$

Noting that $\langle I\rangle^2 = \langle\sigma_x\rangle^2 + \langle\sigma_y\rangle^2 + \langle\sigma_z\rangle^2 = R^2$ is a constant of motion, we define the mean values in a Bloch sphere of radius R: $\langle\sigma_x\rangle = R\sin\theta\cos\phi$, $\langle\sigma_y\rangle = R\sin\theta\sin\phi$, $\langle\sigma_z\rangle = R\cos\theta$, from which we derive the two-state solution

$$|\psi(t)\rangle = e^{i\Phi(t)}\left(\cos\left[\theta(t)/2\right]|\uparrow\rangle + e^{i\phi(t)}\sin\left[\theta(t)/2\right]|\downarrow\rangle\right), \tag{13}$$

where $\Phi(t)$ is the well-known Lewis and Riesenfeld phase, while the coupled Bloch angles θ and ϕ follows from Eq. (12) as

$$\dot{\theta} = -\Delta\,\sin\phi + \Gamma\,(N-1)\sin\theta\,\sin^2\phi, \tag{14a}$$

$$\dot{\phi} = \Omega - \Delta\,\cot\theta\,\cos\phi - \Gamma\,(N-1)\cos\theta\,\sin\phi\,\cos\phi. \tag{14b}$$

From Eq. (13), we compute the mean energy for the representative neuron

$$\epsilon(t) = \frac{1}{2}\left\langle\Omega\sigma_z + \Delta\sigma_x\right\rangle = \frac{\Omega}{2}\,\cos\theta(t) + \frac{\Delta}{2}\,\sin\theta(t)\,\cos\phi(t), \tag{15}$$

and consequently the supercurrent comb intensity

$$\mathcal{I}_N(t) = -N\frac{d\epsilon(t)}{dt} = \Gamma N(N-1)\sin\theta(t)\,\sin^2\phi\left(\frac{\Omega}{2}\sin\theta(t) - \Delta\cos\theta(t)\,\cos\phi(t)\right). \quad (16)$$

In the superradiance phenomenon there are two time intervals associated with the coherently emitted pulse: the characteristic emission time and the delay time, the former being the time width of the emitted pulse and the latter the time interval to attain its maximum intensity. Another distinctive feature of superradiance is the N^2 dependence of the intensity, as shown in Eq. (16). Here, we take advantage of these two time intervals together with the non-linear dependence on N of the intensity to characterize the supercurrent pulses, as analyzed below.

3 Physical parameters and solutions

Recently, Yu *et al.* [97], have estimated the energetic budgets of human neurons by combining metabolic measurements of gray and white matter with morphological data. For excitatory neurons, the energetic demand for maintaining the rest and firing states were quantified as 6.82×10^8 ATP/s and 33.2×10^8 ATP/s, respectively, while the energetic demand of synaptic transmission process was determined to be 15.8×10^8 ATP/s, where ATP/s represents the number of ATP molecules consumed per second. Based on the values presented above and considering a paroxysmal depolarizing shift of 50 milliseconds and a synaptic delay time of 1 millisecond [21], the energy gap between the rest and firing states is given by $8.3 \times 10^{-13}\,J$, while the energy associated with synaptic transmissions becomes $10^{-14}\,J$. We then verify that, in our model, the neuron natural frequency is around $\omega_0 = 1.25$ ZHz, whereas the neuronal coupling is around $g = 15$ EHz. From these values we obtain $g/\omega_0 \simeq 10^{-2}$ with the strong coupling regime obeying the condition $N \gtrsim \omega_0/2g \simeq 50$, which seems unexpectedly easily to satisfy given the exceedingly large number of neurons in the

brain.

Under the above considerations and disregarding the anti-reservoir ($\eta_2 = 0$), we next analyze the seizure spiking by plotting the dimensionless scaled mean energy $\epsilon(t)/\omega_0$ and intensity $\mathcal{I}_N(t)/\gamma\omega_0$ against γt, in the reasonable limit of weak spontaneous firing activity $\Delta/g = 10^{-2}$. By fixing $\Delta = 10\gamma$, what also seems to be a reasonable assumption, and $N = 10^2$, we assume that the representative neuron is initially near the firing state, with $\theta_0 \approx 1/N$ and $\phi_0 = 0$, since the (excited Bloch) state $\theta_0 = \phi_0 = 0$ represents a metastable solution as occurs in Dicke superradiance. In Fig. 2(a) we observe the oscillatory decay of the mean energy to the rest state, as seem from the inset, where the superradiance-like delay time is exactly that in which the energy equals zero: $\tau_D = 1.1 \times 10^{-1}\,\gamma^{-1}$. This oscillatory decay causes the energy in the network to be released as a comb of supercurrent pulses, as shown in Fig. 2(b) where we plot $\mathcal{I}_N(t)/\gamma\omega_0$. This comb of pulses is all contained in an envelop whose scaled duration is around $\gamma\mathcal{T}_N \approx 1/N$, while its scaled intensity is proportional to N^2. However, the scaled time interval of each internal pulse goes as $\gamma\mathcal{T} \approx 1/N^{2.7}$, as indicated in Fig. (2c), where we have pinched off a single supercurrent pulse located at the maximum of the envelope in Fig. 2(b). The comb of supercurrent pulses, with high intensity and short duration, seems to describe very appropriately the rapid oscillations characteristic of the seizure phenomenon. Evidently, these supercurrent envelope, which is remarkably distinguished from Dicke's superradiant pulse, comes basically from the interacting neurons in the strong coupling regime.

(a)

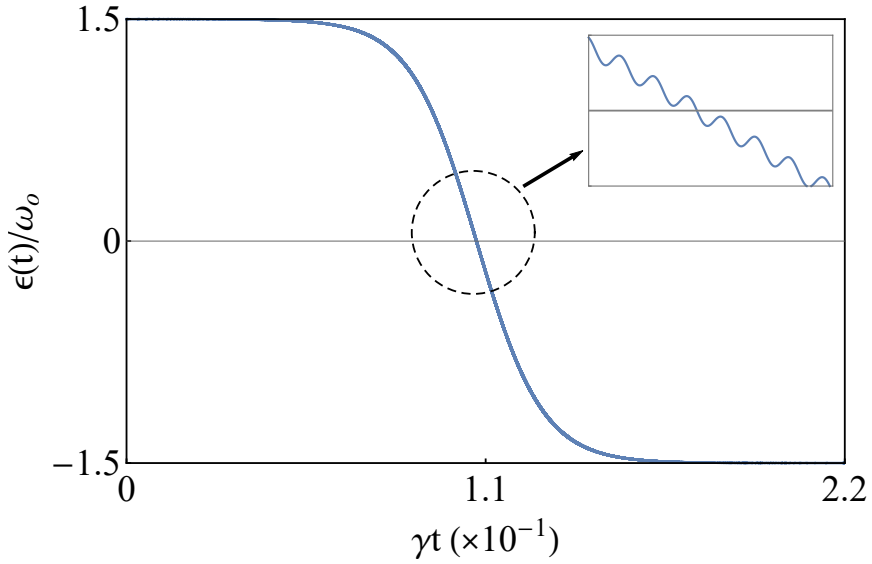
1.5
0
−1.5
0
1.1
2.2
$\epsilon(t)/\omega_o$
$\gamma t\ (\times 10^{-1})$

(b)

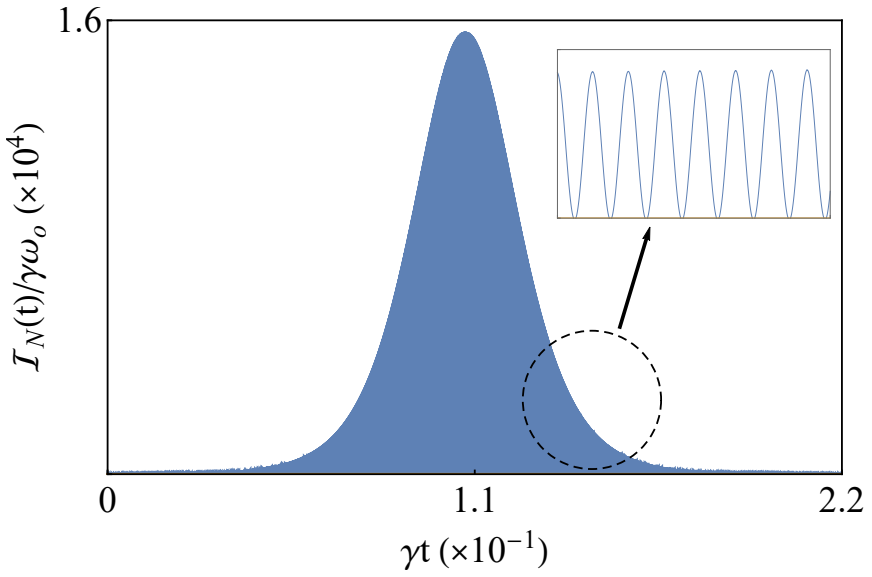
1.6
0
1.1
2.2
$\mathcal{I}_N(t)/\gamma\omega_o\ (\times 10^4)$
$\gamma t\ (\times 10^{-1})$

(c)

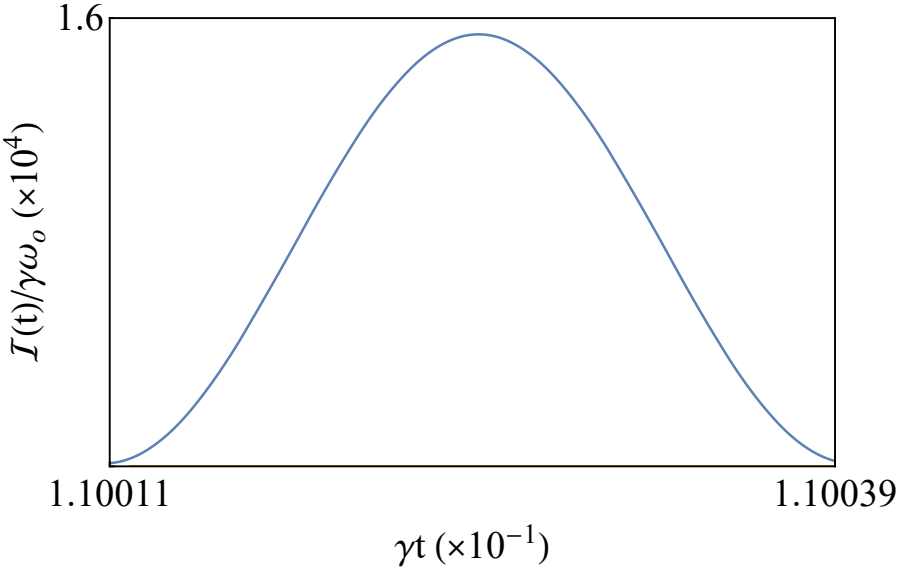

Figure 2: Plot of the (a) scaled mean energy $\epsilon(t)/\omega_0$ and (b) intensity $\mathcal{I}_N(t)/\gamma\omega_0$ against γt, disregarding the anti-reservoir ($\eta_2 = 0$), and considering the weak spontaneous firing activity $\Delta/g = 10^{-2}$, with $g/\omega_0 \simeq 10^{-2}$, $\Delta = 10\gamma$, $N = 10^2$, $\theta_0 \approx 1/N$ and $\phi_0 = 0$. The oscillatory decay of the mean energy to the rest state causes the energy in the network to be released as a comb of supercurrent pulses all contained in an envelop whose scaled duration and intensity are around $\gamma\mathcal{T}_N \approx 1/N$ and N^2. In (c) we plot the intensity $\mathcal{I}(t)/\gamma\omega_0$ against γt for a single supercurrent pulse located at the maximum of the envelope in Fig. 2(b), showing that the scaled time interval of each superpulse goes as $\gamma\mathcal{T} \approx 1/N^{2.7}$.

To demonstrate that the power-law scaling of the emission time and the intensity depends on N, in Fig. 3(a,b) we plot again the scaled mean energy and intensity for $N = 10^3$ —the so far estimated minimum number of neurons in a seizure focus [21]— considering all other parameters as defined in Fig. 2. In this case, the comb of pulses is contained in an envelope of scaled time width $\gamma\mathcal{T}_N \approx 1/N^{1.1}$ and intensity around $N^{2.7}$, with the width of the internal superpulses scaling as $\gamma\mathcal{T} \approx 1/N^2$, as shown in Fig. 3(c), where we have again pinched off the supercurrent pulse located at the maximum of the envelope in Fig. 3(b). Therefore, as N increases, the intensity also increases while the time width of the envelope decreases. The width of the superpulses remains basically the same, $\gamma\mathcal{T} \approx 10^{-6}$, so that the total number of pulses at half height, about 2.5×10^2, is significantly smaller than that for

$N = 10^2$, around 1.2×10^4. This decrease in the number of superpulses with increasing N is another interesting feature of our model, which seems to indicate a brain mechanism to compensate the substantial increase in intensity, for large epileptic focus, in order to avoid possible sequelae from seizures.

(a)

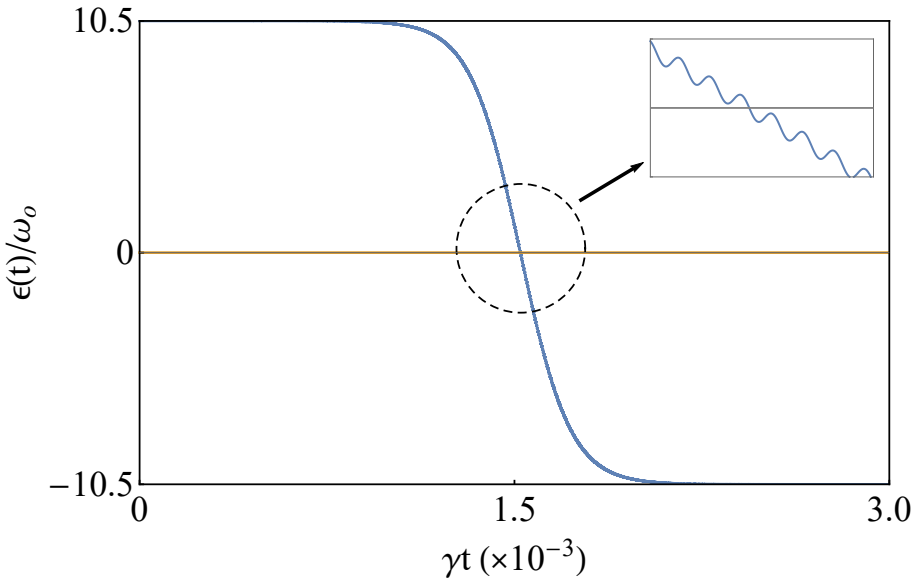

(b)

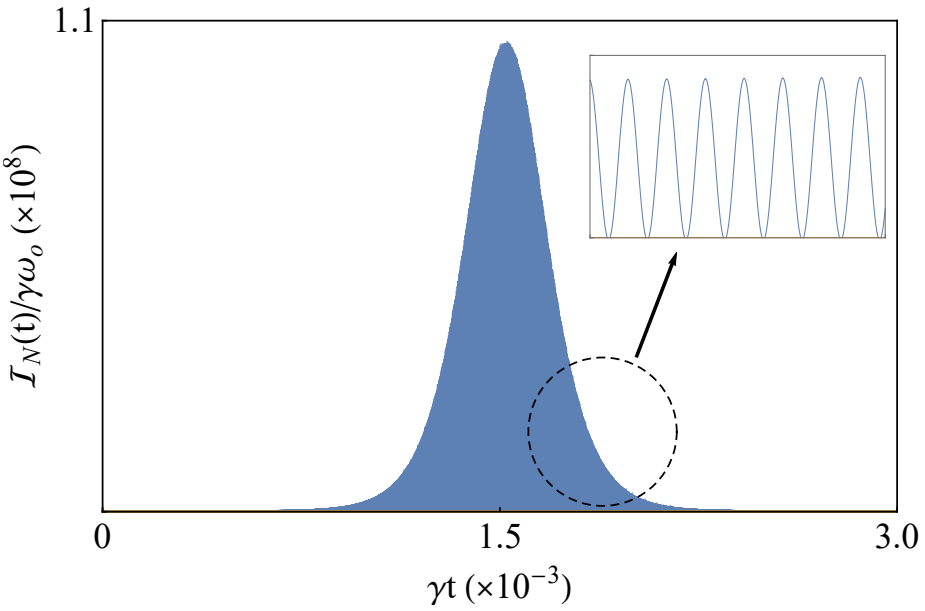

(c)

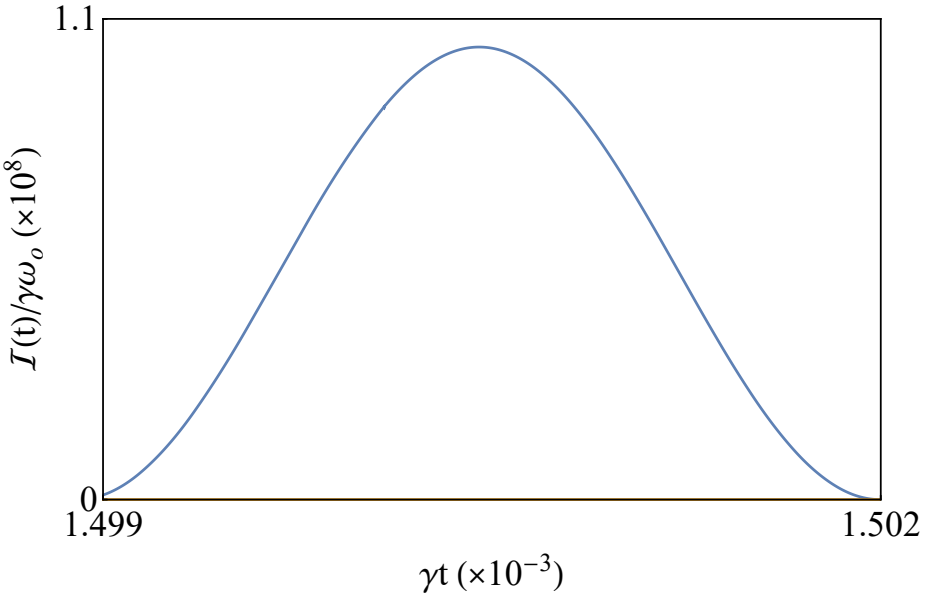

Figure 3: Plot of the (a) scaled mean energy $\epsilon\left(t\right)/\omega_0$ and (b) intensity $\mathcal{I}_N\left(t\right)/\gamma\omega_0$ against γt, considering the same parameters as in Fig. 2, except for $N = 10^3$. The comb of supercurrent pulses are now within an envelop of scaled duration and intensity around $\gamma\mathcal{T}_N \approx 1/N^{1.1}$ and $N^{2.7}$. From the (c) intensity $\mathcal{I}\left(t\right)/\gamma\omega_0$ against γt of a single supercurrent pulse at the maximum of the envelope in Fig. 3(b), we compute the scaled time interval of each internal superpulse as $\gamma\mathcal{T} \approx 1/N^2$.

The same compensation mechanism occurs when we increase the coupling strength to $g/\omega_0 \simeq 10^{-1}$, keeping the same parameters as in Fig. 2. In this case, as shown in Fig. 4, the scaled time width of the envelope, $\gamma\mathcal{T}_N \approx 1/N^{1.2}$, decreases relative to Fig. 2, whereas the scaled intensity increases to N^3. However, as can be verified from Fig. 4(c), we again have around the same width of the estimated 2.5×10^3 internal superpulses at half high, with $\gamma\mathcal{T} \approx 1/N^{2.9} \approx 10^{-6}$.

(a)

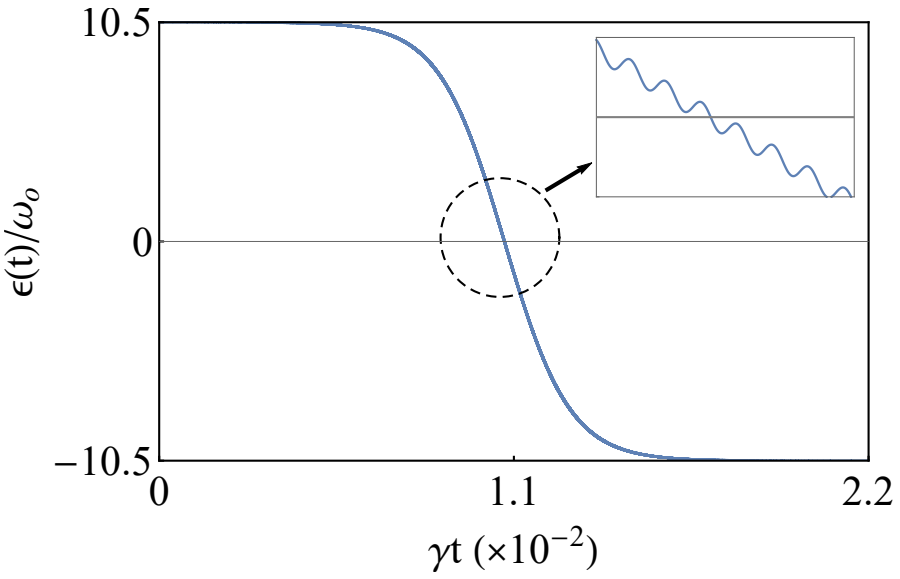

(b)

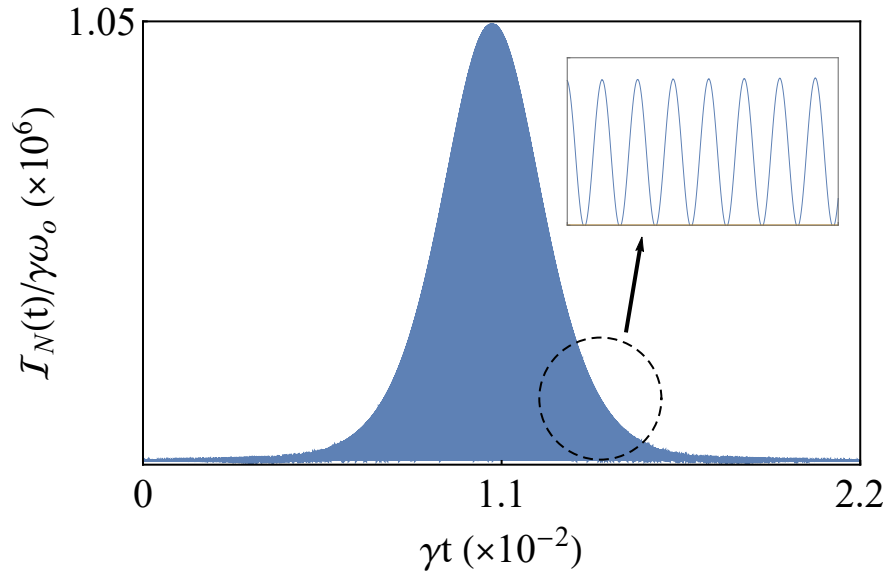

(c)

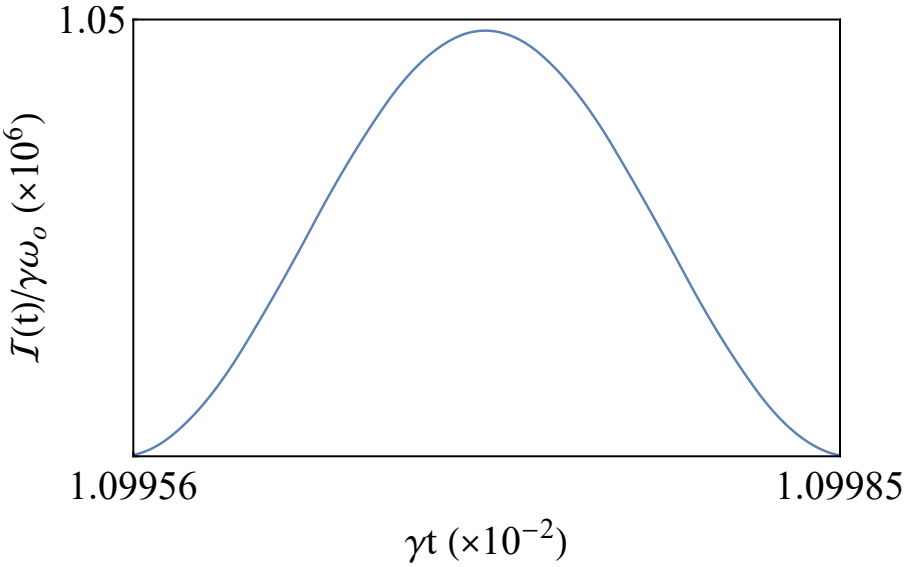

Figure 4: Plot of the (a) scaled mean energy $\epsilon(t)/\omega_0$ and (b) intensity $\mathcal{I}_N(t)/\gamma\omega_0$ against γt, considering the same parameters as in Fig. 2, except for $g/\omega_0 \simeq 10^{-1}$. The scaled time duration and intensity of the envelope of supercurrent pulses goes as $\gamma\mathcal{T}_N \approx 1/N^{1.2}$ and N^3. From the (c) intensity $\mathcal{I}(t)/\gamma\omega_0$ against γt of a single supercurrent pulse located at the maximum of the envelope in Fig. 4(b), we derive the scaled time interval of each internal superpulse as $\gamma\mathcal{T} \approx 1/N^{2.9}$.

When increasing both N and the ratio g/ω_0, considering the values $N = 10^3$ and $g/\omega_0 = 10^{-1}$, keeping all other parameters of Fig. 2, we verify in Fig. 5 that the envelope width decreases more pronouncedly to $\gamma\mathcal{T}_N \approx 1/N^{1.5}$ while the scaled intensity reaches $N^{3.3}$. In this case, we observe only 235 internal superpulses at half high with $\gamma\mathcal{T} \approx 1/N^{2.3} \approx 10^{-7}$, corroborating the brain compensation mechanism by which an increase in the scaled intensity results in fewer supercurrent pulses.

(a)

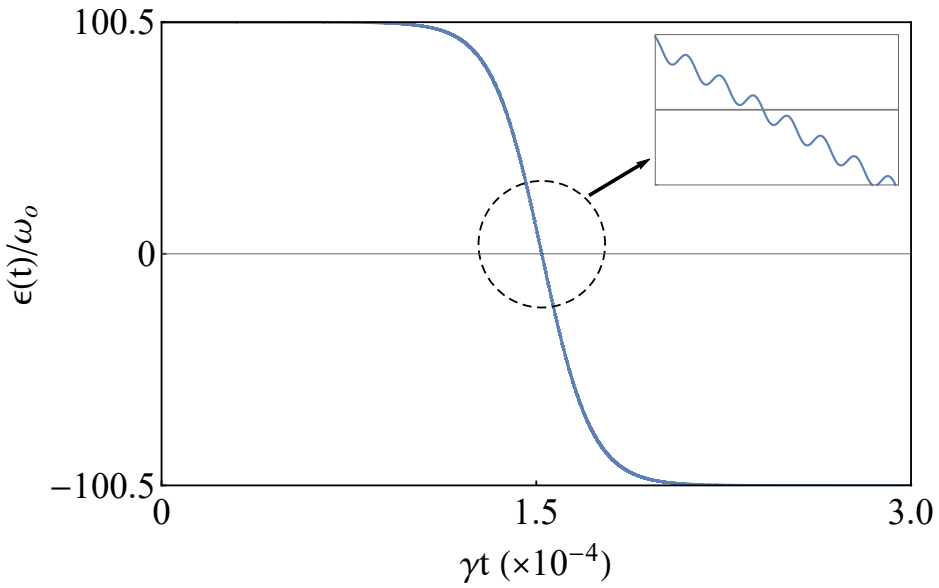

(b)

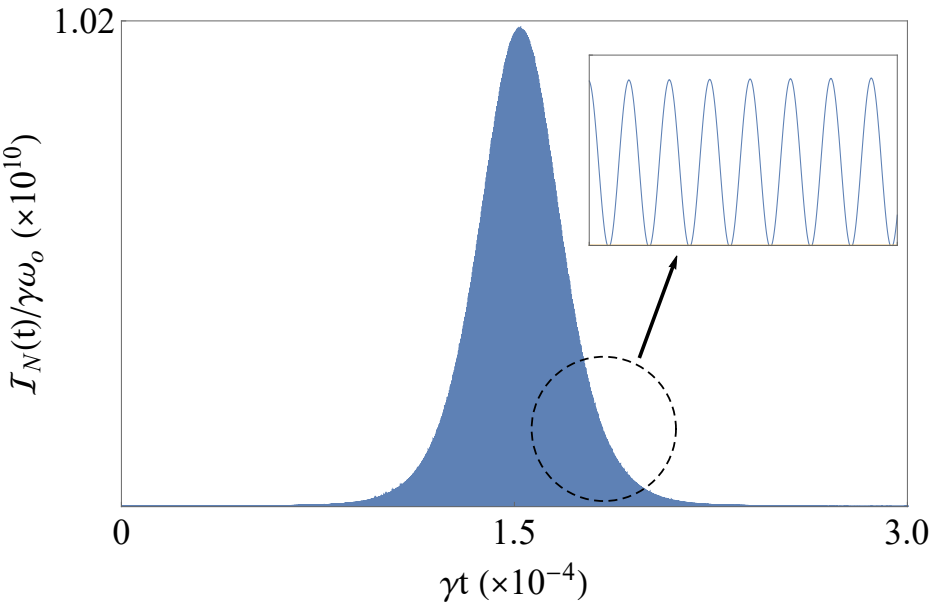

(c)

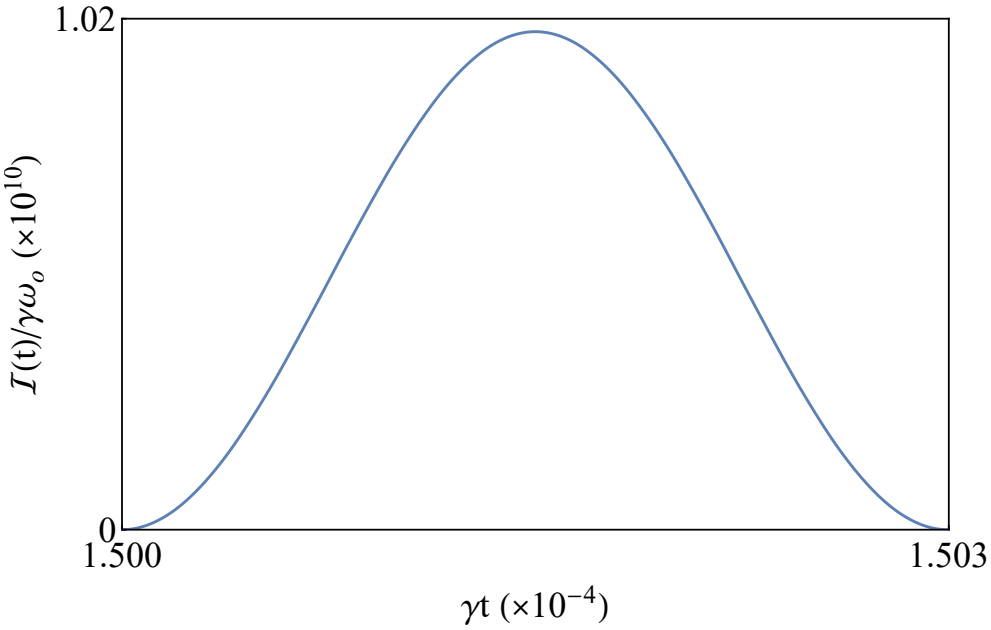

Figure 5: Plot of the (a) scaled mean energy $\epsilon\left(t\right)/\omega_0$ and (b) intensity $\mathcal{I}_N\left(t\right)/\gamma\omega_0$ against γt, considering the same parameters as in Fig. 2, except for $g/\omega_0 \simeq 10^{-1}$ and $N = 10^3$. The scaled time duration and intensity of the envelope of supercurrent pulses goes as $\gamma\mathcal{T}_N \approx 1/N^{1.5}$ and $N^{3.3}$. From the (c) intensity $\mathcal{I}\left(t\right)/\gamma\omega_0$ against γt of a single supercurrent pulse at the maximum of the envelope in Fig. 5(b), we verify that the scaled time interval of each internal superpulse goes as $\gamma\mathcal{T} \approx 1/N^{2.3}$.

Our seizure model based on a network of spin–boson systems, reviews therefore the emergence of a new collective phenomenon characterized by a comb of supercurrent pulses, all contained inside an envelope whose time width, around $1/N\gamma$, is basically that of Dicke's superradiance.

Considering the relaxation time $1/\gamma = 10$ ms, as computed in Ref. [21], we can estimate the duration of a single comb of pulses, which for the case of Fig. 3(b), with $N = 10^3$, leads to the result $\mathcal{T}_N = 2.5$ μs. This time interval is considerably shorter than that of seizures (between 10 s up to 5 min), which leads us to conclude that in a crisis we have the occurrence of a whole sequence of supercurrent combs. Assuming that the time interval between consecutive envelopes is around $10\mathcal{T}_N$, we verify that for a seizure of 10 seconds, the number of envelopes is approximately 4×10^5, while for a 5 minutes crisis we have the occurrence of 1.2×10^7 envelopes.

From Fig. 3(a), we also compute the energy released per neuron in a single comb of supercurrents as around 8.7×10^{-15} J, such that in a seizure of around 1 minute, the energy released in 2.4×10^6 combs is around 2×10^{-8} J, in good agreement with Refs. [21,98,99].

4 Brain mechanisms for disarming seizure

As anticipated above, we thus conclude from our model that seizure is a phenomenon that could occur frequently, since the condition for strong coupling between neurons, $2Ng \gtrsim \omega_0$, is easily achieved. In this regime, the epileptic focus effectively interacts with a single reservoir, a necessary condition for the occurrence of seizures. However, and this is another important conclusion from our model, the action of the anti-reservoir —the remaining neurons around the focus or an external amplification source— becomes decisive to prevent seizure and maintain the normal regime of current transfer. To this end, the coupling

strength between the anti-reservoir and the seizure focus must be strong enough such that $\eta_2 = \alpha N \eta$ with α approaching unity.

We can simulate the seizure disarming, leading to the normal current transfer regime, by considering the whole master equation (10) without neglecting the dissipative effects coming only from the non-diagonal channels. Indeed, in the normal current transfer regime we do not expect for collective processes occurring in a time interval much shorter than Γ^{-1}. Now, from Eq. (10), computing the time-evolving mean values

$$\langle \dot{\sigma_x} \rangle = -\Omega \, \langle \sigma_y \rangle - \Gamma \, \langle \sigma_x \rangle \,, \tag{17}$$

$$\langle \dot{\sigma_y} \rangle = \Omega \, \langle \sigma_x \rangle - \Delta \, \langle \sigma_z \rangle - \Gamma \, (N-1) \, \langle \sigma_y \rangle \, \langle \sigma_z \rangle - \Gamma \, \langle \sigma_y \rangle \,, \tag{18}$$

$$\langle \dot{\sigma_z} \rangle = \Delta \, \langle \sigma_y \rangle + \Gamma \, (N-1) \, \langle \sigma_y \rangle^2 - \Gamma \, (\langle \sigma_z \rangle - 1) \,, \tag{19}$$

and assuming the state $|\psi \, (t)\rangle$ of Eq. (13), we obtain, instead of Eqs. (14), the solution

$$\dot{\theta} = -\Delta \, \sin \phi + \Gamma \, (N-1) \sin \theta \, \sin^2 \phi + \Gamma \, (\cot \theta - \csc \theta) \,, \tag{20a}$$

$$\dot{\phi} = \Omega - \Delta \, \cot \theta \, \cos \phi - \Gamma \, (N-1) \cos \theta \, \sin \phi \, \cos \phi. \tag{20b}$$

In Fig. 6, we plot $\mathcal{I}_N \, (t) \, / \gamma \omega_0$ against γt, considering the same parameters as in Fig. 2 with $\alpha = 0.4$ (a), $\alpha = 0.8$ (b) and $\alpha = 0.996$ (c). We still observe seizure for $\alpha = 0.4$, with

scaled intensity and time duration around N^2 and $\gamma\mathcal{T}_N \approx 1/N$. For $\alpha = 0.8$, the seizure intensity decreases to around $N^{1.8}$ while the time width increases to $\gamma\mathcal{T}_N \approx 1/N^{0.4}$. This weakened seizure scenario persists until around $\alpha = 0.996$, when we reach the normal current transfer regime —analogous to the fluorescence emission in atomic optics— with the scaled intensity and time width being N and $1/\gamma$. Similarly to the seizure regime, we also have a comb of pulses each with time width $\gamma\mathcal{T} \approx 1/N^{2.5} = 10^{-5}$, an order of magnitude greater than the time width of the pulses in Fig. 2(b). However, the number of pulses in Fig. 6(c), approximately 10^6, is about two orders of magnitude higher than in Fig. 2(b); this increase arises because the time width in Fig. 6(c) is five orders of magnitude larger than that in Fig. 2(c). Finally, we note that in the seizure regime, the comb of pulses occurs at time intervals at least an order of magnitude shorter than the relaxation time $1/\gamma$. In contrast, in the normal current transfer regime of Fig. 6(c), the comb of pulses is released at a time interval approximately 50 times longer than the relaxation time.

We emphasize that our analogy between the seizure and normal current transfer regimes with the phenomena of fluorescence and superradiance considers only the envelopes of the combs of currents. The internal pulses occurring in both regimes represent a new phenomenon, emerging as a consequence of strong coupling between neurons.

(a)

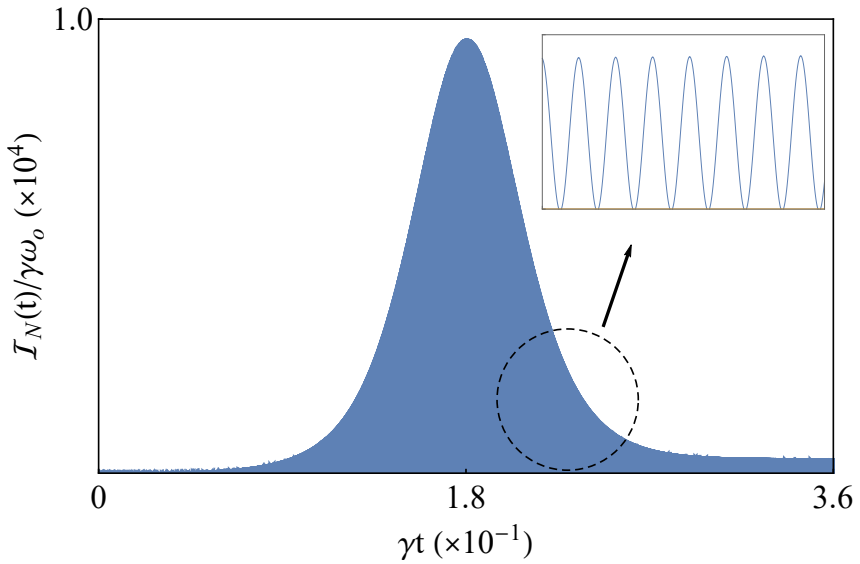
1.0
$I_N(t)/\gamma\omega_o$ ($\times 10^4$)
0
1.8
3.6
γt ($\times 10^{-1}$)

(b)

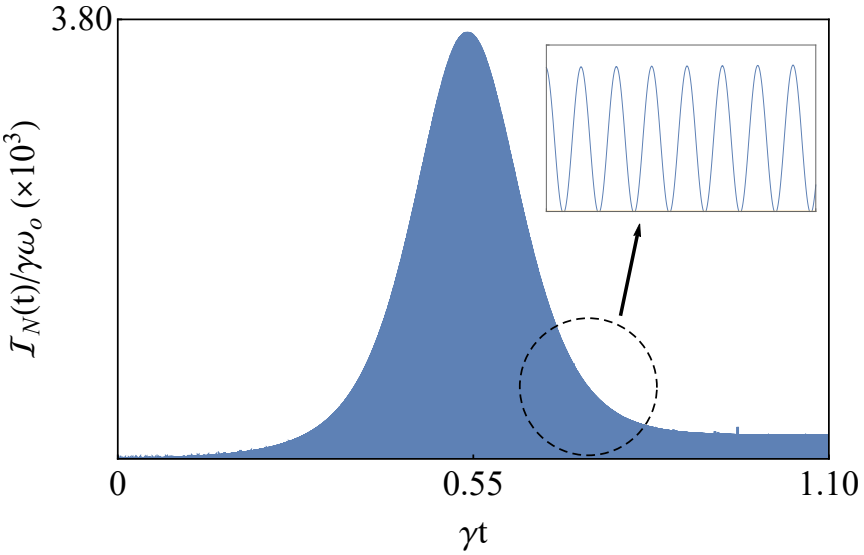
3.80
$I_N(t)/\gamma\omega_o$ ($\times 10^3$)
0
0.55
1.10
γt

(c)

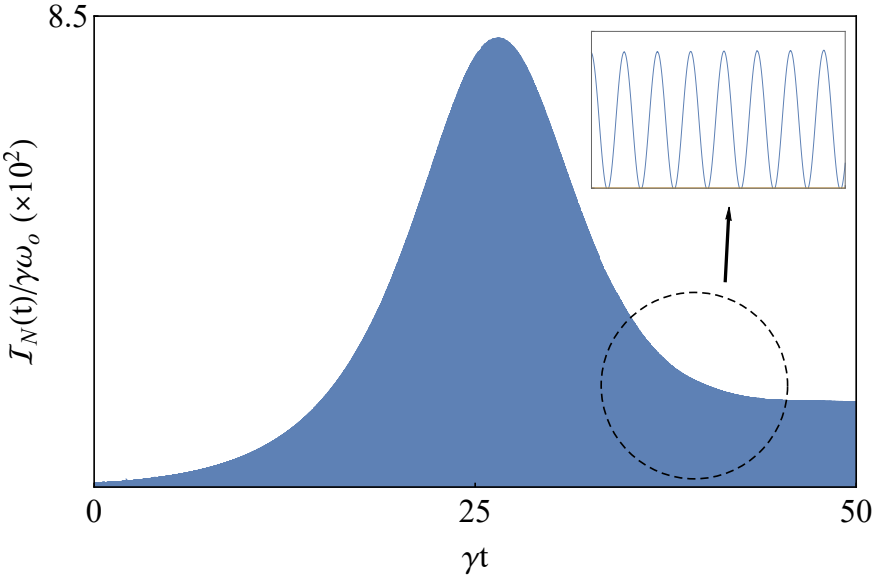

Figure 6: Plot of the scaled intensity $\mathcal{I}_N(t)/\gamma\omega_0$ against γt, considering the same parameters as in Fig. 2 with $\alpha = 0.4$ (a), $\alpha = 0.8$ (b) and $\alpha = 0.996$ (c). The normal current transfer regime is reached in (c) when the scaled intensity and time width becomes proportional to N and $1/\gamma$.

For the relaxation time $1/\gamma = 10$ ms advanced above, we obtain from the maximum intensity per neuron in Fig. 6(c), the value $\mathcal{I}_{max} = 7 \times 10^{-8}$ J/s, which lies in the range $10^{-9} - 10^{-6}$ J/s in accordance with Refs. [21,98,99]. In fact, from the input of experimental data —as the transition energy between the rest and firing states (ω_0) and the energetic demand of synaptic transmission process (g)— together with the theoretically computed value for the relaxation rate (γ), our model is able to provide a quite reasonable result for the rate of energy produced by a neuron in the normal current transfer regime.

By defining a "quality factor" for the neuron similar to that of a resonator, $Q = \omega_0/\gamma$, we compute from our input parameters the remarkable value $Q \approx 10^{17}$, which seems to corroborate our above hypothesis that the non-local tunneling may indeed be the phenomenon supporting the description of the firing process in a neuron by the spin–boson system.

In the case where the coupling strength between the neurons inside and outside the

seizure focus is not strong enough to disarm seizure, an external anti-reservoir can be considered as suggested in Ref. [91], in a technique known as epidural dorsal column stimulation (DCS). The DCS represents a potential non-invasive therapeutic approach for neurological disorders, distinct from conventional drug-based treatments, and has demonstrated promising results [100]. For individuals with Parkinson's disease, numerous clinical investigations have identified abnormal elevations in synchronized oscillatory neuronal activity in the basal ganglia [90,101]. In 2017, the effects of DCS for Parkinson's disease were reported by Yadav *et al.* [91], suggesting that electrical stimulation of the dorsal column fibers could lead to the desynchronization of cortico-striatal activity. Human trials were conducted utilizing this technique, which reported favorable clinical effects of DCS [102,103]. These effects extend beyond the amelioration of motor symptoms associated with akinesia, bradykinesia, and tremor, offering substantial relief for axial symptoms, impairments in gait and posture, which present significant challenges when using existing therapeutic options.

Another way to disarm seizure is to increase the tunneling rate Δ to around the coupling g. Back to Eq. (16) and considering the same parameters as in Fig. 2, except for $\Delta/g = 1$, in Fig. 7 we plot the scaled intensity $\mathcal{I}_N(t)/\gamma\omega_0$ against γt. We observe that this intensity decreases from around N to around zero in a time interval of about $1/10\gamma$. Therefore, a high tunneling frequency, which increases the population inversion rate of each neuron, gets rid of the synchronized exchange of excitation in the network, and consequently of the collective effects leading to the supercurrents.

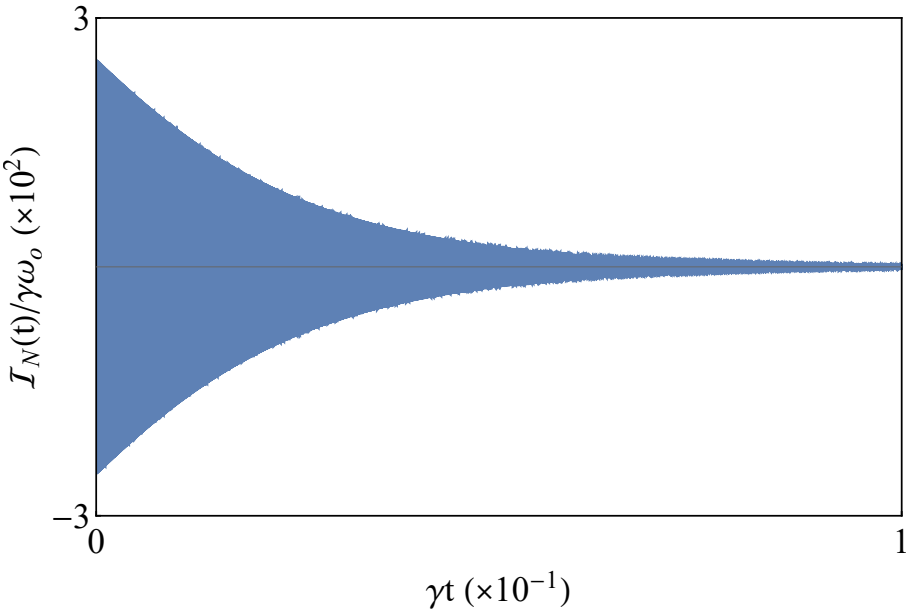

Figure 7: Plot of the scaled intensity $\mathcal{I}_N(t)/\gamma\omega_0$ against γt, considering the same parameters as in Fig. 2, except for $\Delta/g = 1$, showing that the enhanced tunneling mechanism may disarm seizure.

A set of factors contribute to enhance the tunneling frequency Δ, driving the neuron's spontaneous activity in the absence of direct external stimuli. Random synaptic inputs and channel noise as well as membrane potential fluctuations [104,105], driven by the balance of ion flows, can bring the neuron to a threshold that triggers spontaneous activity. Moreover, neuromodulators like dopamine, serotonin, and acetylcholine also play a role by altering the neuron's excitability, making it more prone to firing [106]. We finally mention that the reservoir temperature can affect membrane properties and ion channel kinetics, while metabolic factors, such as fluctuations in ATP levels, can disrupt ionic gradients and lead to spontaneous action potentials [98].

Conclusions

Reasoning by analogy to the OBH model for electron transfer in chemical reactions, here we present a quantum description of the firing process in a neuron. To this end, we conjecture that the firing mechanism, as well as the electron transfer in the OBH treatment, can be described by the spin–boson model. We support our conjecture by means of reasonable physical arguments and by considering the phenomenon of non-local tunneling [86], a highly probable process effectively shielded from dissipation effects. With this, we describe the neural network as a set of interconnected spin–boson units, to obtain the master equation ruling the network dynamics using the Holstein-Primakoff and mean-field approximations. A convulsive crisis occurs when the coupling between neurons is strong enough so that the entire seizure focus interacts effectively with a single thermal reservoir.

Our main result consists in the description of seizure as an emergent collective effect by which the network emits a sequence of supercurrents envelopes. The time width and intensity of these envelopes, of the order of $1/N^u\gamma$, and intensity proportional to N^v, with real $u, v > 1$, bears a strong resemblance to the time width of a superradiant pulse in atomic optics. However, in superradiance we do not have the internal pulses inside these envelopes, so that these superpulses, whose width is of the order of N times smaller than that of the envelope, seem to be a singular effect characterizing seizure.

We note that in the absence of seizure, or in the normal current transfer regime, the intensity and the time width of the envelope becomes proportional to N and $1/\gamma$, which is equivalent to the phenomenon of fluorescence in atomic optics where the internal pulses are also absent. Therefore, we describe seizure as a phase transition that bears similarity to the second-order transition between fluorescence and superradiance in atomic optics. We believe that this characterization of seizure as a phase transition contributes to justify our quantum approach as much as the results we have estimated in good agreement with the experimental data presented in neuroscience literature. From the input of experimental data,

such as the energy gap between the rest and firing state, the energy associated with synaptic transmissions, and the relaxation time of a neuron, we are able to estimate the maximum intensity produced per neuron in the normal current transfer regime, the energy released by a neuron in a 1 minute seizure, and the time interval of a single comb of supercurrents.

We stress that our quantum model for seizure is not based on the phenomenon of phase coherence of superposition states, which is readily eliminated by the noise introduced by both the reservoir and the anti-reservoir [107]. However, our approach demands the quantum coherence of the emergent collective effects leading to superradiance-like phase transition.

Another worthy conclusion from our model is that the seizure mechanism can be disarmed through the action of an anti-reservoir which can be played by the remaining neurons around the focus or an external amplification source. The enhancement of the tunneling rate Δ associated with the spontaneous neuronal activity can also be used to disarm seizure, and we have listed some factors that can stimulate this spontaneous activity.

Finally, we observe that our neural network model allows us to describe the mechanism of seizure within a framework that is considerably broader than that offered by conventional biophysical models, such as those based on the Hodgkin–Huxley formalism. Indeed, in our quantum mechanical framework, the seizure is understood as a phase transition from an incoherent process to a coherent collective one. Within this phase transition, we have access to a wide range of analytical tools that enable a more precise characterization and deeper understanding of the seizure, including the average energy, intensity, and characteristic timescale of the supercurrent pulses.

References

[1] Onuchic, J. N. et al. Some aspects of electron-transfer reaction dynamics. The Journal of Physical Chemistry, v. 90, n. 16, p. 3707-3721, 1986.

[2] Uhlhaas, P. J.; Singer, W. Neuronal dynamics and neuropsychiatric disorders: toward a translational paradigm for dysfunctional large-scale networks. Neuron, v. 75, n. 6, p. 963-980, 2012.

[3] van P. M. Dynamics of neural networks: A Mathematical and Clinical Approach. Springer Berlin Heidelberg; 2020.

[4] Wei, L. et al. Functional connectivity–based prediction of global cognition and motor function in riluzole-naive amyotrophic lateral sclerosis patients. Network Neuroscience, v. 6, n. 1, p. 161-174, 2022.

[5] El Houssaini, K. et al. Seizures, refractory status epilepticus, and depolarization block as endogenous brain activities. Physical Review E, v. 91, n. 1, p. 010701, 2015.

[6] Safi, K. et al. Bigger is not always better: when brains get smaller. Biology Letters, v. 1, n. 3, p. 283-286, 2005.

[7] Buzsaki, G. Rhythms of the Brain. Oxford university press, 2006.

[8] Foster, A. C.; Kemp, J. A. Glutamate-and GABA-based CNS therapeutics. Current opinion in pharmacology, v. 6, n. 1, p. 7-17, 2006.

[9] Gerstner, W.; Kistler, W. M. Spiking neuron models: Single neurons, populations, plasticity. Cambridge university press, 2002.

[10] Dayan, P.; Abbott, L. F. Theoretical neuroscience: computational and mathematical modeling of neural systems. MIT press, 2005.

[11] Tsien, J. Z. et al. On initial brain activity mapping of episodic and semantic memory code in the hippocampus. Neurobiology of learning and memory, v. 105, p. 200-210, 2013.

[12] Barnett, M. W.; Larkman, P. M. The action potential. Practical neurology, v. 7, n. 3, p. 192-197, 2007.

[13] Buzsaki, G. The brain from inside out. Oxford University Press, USA, 2019.

[14] Clayton, D. F. The genomic action potential. Neurobiology of learning and memory, v. 74, n. 3, p. 185-216, 2000.

[15] Lodato, S.; Arlotta, P. Generating neuronal diversity in the mammalian cerebral cortex. Annual review of cell and developmental biology, v. 31, n. 1, p. 699-720, 2015.

[16] Bear, M. et al. Neuroscience: exploring the brain, enhanced edition: exploring the brain. Jones & Bartlett Learning, 2020.

[17] Clements, J. D. Transmitter timecourse in the synaptic cleft: its role in central synaptic function. Trends in neurosciences, v. 19, n. 5, p. 163-171, 1996.

[18] Harris, K. D.; Shepherd, G. M. The neocortical circuit: themes and variations. Nature neuroscience, v. 18, n. 2, p. 170-181, 2015.

[19] Sumadewi, K. T. et al. Biomolecular mechanisms of epileptic seizures and epilepsy: a review. Acta Epileptologica, v. 5, n. 1, p. 28, 2023.

[20] Jefferys, J. G. Advances in understanding basic mechanisms of epilepsy and seizures. Seizure, v. 19, n. 10, p. 638-646, 2010.

[21] Kandel, E. R. et al. (Ed.). Principles of neural science. New York: McGraw-hill, 2000.

[22] Laryushkin, D. P. et al. Of the mechanisms of paroxysmal depolarization shifts: generation and maintenance of bicuculline-induced paroxysmal activity in rat hippocampal cell cultures. International Journal of Molecular Sciences, v. 24, n. 13, p. 10991, 2023.

[23] Laryushkin, D. P. et al. Role of L-type voltage-gated calcium channels in epileptiform activity of neurons. International Journal of Molecular Sciences, v. 22, n. 19, p. 10342, 2021.

[24] Zhou, Y.; Danbolt, N. C. Glutamate as a neurotransmitter in the healthy brain. Journal of neural transmission, v. 121, p. 799-817, 2014.

[25] Shen, W. et al. Can glial cells save neurons in epilepsy?. Neural Regeneration Research, v. 18, n. 7, p. 1417-1422, 2023.

[26] Shah, M. M. et al. Seizure-induced plasticity of h channels in entorhinal cortical layer III pyramidal neurons. Neuron, v. 44, n. 3, p. 495-508, 2004.

[27] Shruti, S. et al. A seizure-induced gain-of-function in BK channels is associated with elevated firing activity in neocortical pyramidal neurons. Neurobiology of disease, v. 30, n. 3, p. 323-330, 2008.

[28] de Lanerolle, N. C. et al. Astrocytes and epilepsy. Neurotherapeutics, v. 7, p. 424-438, 2010.

[29] Tian, G. F. et al. An astrocytic basis of epilepsy. Nature medicine, v. 11, n. 9, p. 973-981, 2005.

[30] Magloire, V. et al. GABAergic interneurons in seizures: investigating causality with optogenetics. The Neuroscientist, v. 25, n. 4, p. 344-358, 2019.

[31] Carlen, P. L. et al. The role of gap junctions in seizures. Brain research reviews, v. 32, n. 1, p. 235-241, 2000.

[32] Velazquez, J. L. P.; Carlen, P. L. Gap junctions, synchrony and seizures. Trends in neurosciences, v. 23, n. 2, p. 68-74, 2000.

[33] Raimondo, J. V. et al. Ion dynamics during seizures. Frontiers in cellular neuroscience, v. 9, p. 419, 2015.

[34] Cohen, I. et al. On the origin of interictal activity in human temporal lobe epilepsy in vitro. Science, v. 298, n. 5597, p. 1418-1421, 2002.

[35] Timofeev, I. et al. The role of chloride-dependent inhibition and the activity of fast-spiking neurons during cortical spike–wave electrographic seizures. Neuroscience, v. 114, n. 4, p. 1115-1132, 2002.

[36] Bazhenov, M. et al. Cellular and network mechanisms of electrographic seizures. Drug Discovery Today: Disease Models, v. 5, n. 1, p. 45-57, 2008.

[37] Ngomba, R. T. et al. Positive allosteric modulation of metabotropic glutamate 4 (mGlu4) receptors enhances spontaneous and evoked absence seizures. Neuropharmacology, v. 54, n. 2, p. 344-354, 2008.

[38] Loddenkemper, T. et al. Continuous spike and waves during sleep and electrical status epilepticus in sleep. Journal of Clinical Neurophysiology, v. 28, n. 2, p. 154-164, 2011.

[39] Wong, M. Modulation of dendritic spines in epilepsy: cellular mechanisms and functional implications. Epilepsy & Behavior, v. 7, n. 4, p. 569-577, 2005.

[40] Dudek, F. E.; Sutula, T. P. Epileptogenesis in the dentate gyrus: a critical perspective. Progress in brain research, v. 163, p. 755-773, 2007.

[41] Hanada, T. Ionotropic glutamate receptors in epilepsy: a review focusing on AMPA and NMDA receptors. Biomolecules, v. 10, n. 3, p. 464, 2020.

[42] Jensen, F. E. The role of glutamate receptor maturation in perinatal seizures and brain injury. International Journal of Developmental Neuroscience, v. 20, n. 3-5, p. 339-347, 2002.

[43] Zamponi, G. W. et al. Role of voltage-gated calcium channels in epilepsy. Pflügers Archiv-European Journal of Physiology, v. 460, p. 395-403, 2010.

[44] Khosravani, H.; Zamponi, G. W. Voltage-gated calcium channels and idiopathic generalized epilepsies. Physiological reviews, v. 86, n. 3, p. 941-966, 2006.

[45] Perea, G. et al. Activity-dependent switch of GABAergic inhibition into glutamatergic excitation in astrocyte-neuron networks. Elife, v. 5, p. e20362, 2016.

[46] Bugaysen, J. et al. Continuous modulation of action potential firing by a unitary GABAergic connection in the globus pallidus in vitro. Journal of Neuroscience, v. 33, n. 31, p. 12805-12809, 2013.

[47] Gonzales-Islas, C. et al. GABAergic synaptic scaling is triggered by changes in spiking activity rather than AMPA receptor activation. Elife, v. 12, p. RP87753, 2024.

[48] Abed Zadeh, A. et al. Non-monotonic effects of GABAergic synaptic inputs on neuronal firing. PLoS computational biology, v. 18, n. 6, p. e1010226, 2022.

[49] Zeng, L. H. et al. Kainate seizures cause acute dendritic injury and actin depolymerization in vivo. Journal of Neuroscience, v. 27, n. 43, p. 11604-11613, 2007.

[50] Trevelyan, A. J.; Schevon, C. A. How inhibition influences seizure propagation. Neuropharmacology, v. 69, p. 45-54, 2013.

[51] Cremer, C. M. et al. Pentylenetetrazole-induced seizures affect binding site densities for GABA, glutamate and adenosine receptors in the rat brain. Neuroscience, v. 163, n. 1, p. 490-499, 2009.

[52] Liu, J. et al. A sensitive and specific nanosensor for monitoring extracellular potassium levels in the brain. Nature Nanotechnology, v. 15, n. 4, p. 321-330, 2020.

[53] Blank, L. J. et al. Neurodegenerative disease is associated with increased incidence of epilepsy: a population based study of older adults. Age and ageing, v. 50, n. 1, p. 205-212, 2021.

[54] Simonet, C. et al. Assessment of risk factors and early presentations of Parkinson disease in primary care in a diverse UK population. JAMA neurology, v. 79, n. 4, p. 359-369, 2022.

[55] Vossel, K.; Karageorgiou, E. Silent Seizures and Memory Loss in Alzheimer's Disease. Frontiers in Neurology, v. 12, p. 648650, 2021.

[56] Thakor, B. et al. Juvenile Huntington's disease masquerading as progressive myoclonus epilepsy. Epilepsy & Behavior Reports, v. 16, p. 100470, 2021.

[57] Sarella, P. N. K. et al. Pharmacological and Non-pharmacological Management of Bipolar Disorder with Comorbid Huntington's Disease: A Case Report. Journal of Clinical and Pharmaceutical Research, p. 5-8, 2023.

[58] Zhang, D. et al. SLC2A1 variants cause late-onset epilepsy and the genetic-dependent stage feature: For the China Epilepsy Gene 1.0 Project. Acta Epileptologica, v. 6, n. 1, p. 38, 2024.

[59] de Melo, I. S. et al. Modulation of glucose availability and effects of hypo-and hyperglycemia on status epilepticus: what we do not know yet?. Molecular Neurobiology, v. 58, p. 505-519, 2021.

[60] Kiani, L. Blood–brain barrier disruption following seizures. Nature Reviews Neurology, v. 19, n. 4, p. 196-196, 2023.

[61] Cudna, A. et al. Changes in serum blood-brain barrier markers after bilateral tonic-clonic seizures. Seizure: European Journal of Epilepsy, v. 106, p. 129-137, 2023.

[62] Bronisz, E. et al. Serum Proteins Associated with Blood–Brain Barrier as Potential Biomarkers for Seizure Prediction. International Journal of Molecular Sciences, v. 23, n. 23, p. 14712, 2022.

[63] Wood, H. Seizures induce NLRP3 inflammasome signalling. Nature Reviews Neurology, v. 18, n. 10, p. 575-575, 2022.

[64] Ye, X. G. et al. Increased expression of NLRP3 associated with elevated levels of HMGB1 in children with febrile seizures: a case–control study. BMC pediatrics, v. 24, n. 1, p. 44, 2024.

[65] Qin, Z. et al. GPR120 modulates epileptic seizure and neuroinflammation mediated by NLRP3 inflammasome. Journal of Neuroinflammation, v. 19, n. 1, p. 121, 2022.

[66] Zsurka, G.; Kunz, W. S. Mitochondrial dysfunction and seizures: the neuronal energy crisis. The Lancet Neurology, v. 14, n. 9, p. 956-966, 2015.

[67] Kovács, R. et al. Bioenergetic mechanisms of seizure control. Frontiers in Cellular Neuroscience, v. 12, p. 335, 2018.

[68] Pearson-Smith, J. N.; Patel, M.. Metabolic dysfunction and oxidative stress in epilepsy. International Journal of Molecular Sciences, v. 18, n. 11, p. 2365, 2017.

[69] Löwdin, P. O. Proton tunneling in DNA and its biological implications. Reviews of Modern Physics, v. 35, n. 3, p. 724, 1963.

[70] Mohseni, M. et al. (Ed.). Quantum effects in biology. Cambridge University Press, 2014.

[71] Zinth, W.; Wachtveitl, J. The first picoseconds in bacterial photosynthesis—ultrafast electron transfer for the efficient conversion of light energy. ChemPhysChem, v. 6, n. 5, p. 871-880, 2005.

[72] O'Reilly, E. J.; Olaya-Castro, A. Non-classicality of the molecular vibrations assisting exciton energy transfer at room temperature. Nature communications, v. 5, n. 1, p. 3012, 2014.

[73] Fleming, G. R.; Scholes, G. D. Quantum mechanics for plants. Nature, v. 431, n. 7006, p. 256-257, 2004.

[74] Page, C. C. et al. Leslie. Mechanism for electron transfer within and between proteins. Current opinion in chemical biology, v. 7, n. 5, p. 551-556, 2003.

[75] Bendall, D. S. Interprotein electron transfer. In: Protein electron transfer. Garland Science, 2020. p. 43-68.

[76] Sia, P. I. et al. Quantum biology of the retina. Clinical & Experimental Ophthalmology, v. 42, n. 6, p. 582-589, 2014.

[77] Ganim, Ziad et al. Vibrational excitons in ionophores: Experimental probes for quantum coherence-assisted ion transport and selectivity in ion channels. New Journal of Physics, v. 13, n. 11, p. 113030, 2011.

[78] Sanchez, H.; Moussa, M. H. Y. Amplificative–dissipative tunneling: the problem of genetic mutation. Eur. Phys. J. Plus 139, 888 (2024).

[79] Breakspear, M. et al. A unifying explanation of primary generalized seizures through nonlinear brain modeling and bifurcation analysis. Cerebral Cortex, v. 16, n. 9, p. 1296-1313, 2006.

[80] Cressman, J. R. et al. The influence of sodium and potassium dynamics on excitability, seizures, and the stability of persistent states: I. Single neuron dynamics. Journal of computational neuroscience, v. 26, p. 159-170, 2009.

[81] Terry, J. R. et al. Seizure generation: the role of nodes and networks. Epilepsia, v. 53, n. 9, p. e166-e169, 2012.

[82] Jirsa, V. K. et al. On the nature of seizure dynamics. Brain, v. 137, n. 8, p. 2210-2230, 2014.

[83] Hameroff, S.; Penrose, R. Orchestrated reduction of quantum coherence in brain microtubules: A model for consciousness. Mathematics and computers in simulation, v. 40, n. 3-4, p. 453-480, 1996.

[84] Kerskens, C. M.; Pérez, D. L. Experimental indications of non-classical brain functions. Journal of Physics Communications, v. 6, n. 10, p. 105001, 2022.

[85] Leggett, A. J. et al. Dynamics of the dissipative two-state system. Reviews of Modern Physics, v. 59, n. 1, p. 1, 1987.

[86] Neto, G. D. M. et al. Nonlocal dissipative tunneling for high-fidelity quantum-state transfer between distant parties. Physical Review A—Atomic, Molecular, and Optical Physics, v. 85, n. 5, p. 052303, 2012.

[87] Dicke, R. H. Coherence in spontaneous radiation processes. Physical review, v. 93, n. 1, p. 99, 1954.

[88] Rulkov, N. F. et al. Oscillations in large-scale cortical networks: map-based model. Journal of computational neuroscience, v. 17, p. 203-223, 2004.

[89] Fröhlich, F. et al. Slow state transitions of sustained neural oscillations by activity-dependent modulation of intrinsic excitability. Journal of Neuroscience, v. 26, n. 23, p. 6153-6162, 2006.

[90] Yadav, A. P. et al. Chronic spinal cord electrical stimulation protects against 6-hydroxydopamine lesions. Scientific reports, v. 4, n. 1, p. 3839, 2014.

[91] Yadav, A. P.; Nicolelis, M. Electrical stimulation of the dorsal columns of the spinal cord for Parkinson's disease. Movement Disorders, v. 32, n. 6, p. 820-832, 2017.

[92] Primakoff, H.; Holstein, T. Many-body interactions in atomic and nuclear systems. Physical Review, v. 55, n. 12, p. 1218, 1939.

[93] Caldeira, A. O.; Leggett, A. J. Path integral approach to quantum Brownian motion. Physica A: Statistical mechanics and its Applications, v. 121, n. 3, p. 587-616, 1983.

[94] de Ponte, M. A. et al. Networks of dissipative quantum harmonic oscillators: A general treatment. Physical Review A—Atomic, Molecular, and Optical Physics, v. 76, n. 3, p. 032101, 2007.

[95] Mizrahi, S. S.; Mewes, M. A. Pulsed superradiant emission from a magnetic dipole system. International Journal of Modern Physics B, v. 7, n. 12, p. 2353-2365, 1993.

[96] Mizrahi, S. S. May the atomic superradiant emission be described by a single-particle mean-field Hamiltonian?. Physics Letters A, v. 144, n. 6-7, p. 282-286, 1990.

[97] Yu, Y. et al. Evaluating the gray and white matter energy budgets of human brain function. Journal of Cerebral Blood Flow & Metabolism, v. 38, n. 8, p. 1339-1353, 2018.

[98] Hille, B. Ion Channels of Excitable Membranes. 3rd ed. Sunderland: Sinauer Associates, 2001.

[99] Hyder, F. et al. Cortical energy demands of signaling and non-signaling components in brain function and disease. Proceedings of the National Academy of Sciences, v. 110, n. 9, p. 3549-3554, 2013.

[100] de Andrade, E. M. et al. Spinal cord stimulation for Parkinson's disease: a systematic review. Neurosurgical review, v. 39, p. 27-35, 2016.

[101] Brown, P. Oscillatory nature of human basal ganglia activity: relationship to the pathophysiology of Parkinson's disease. Movement disorders: official journal of the Movement Disorder Society, v. 18, n. 4, p. 357-363, 2003.

[102] Thiriez, C. et al. Spinal stimulation for movement disorders. Neurotherapeutics, v. 11, n. 3, p. 543-552, 2014.

[103] Thevathasan, W. et al. Spinal cord stimulation failed to relieve akinesia or restore locomotion in Parkinson disease. Neurology, v. 74, n. 16, p. 1325-1327, 2010.

[104] Manwani, A. et al. Channel noise in excitable neural membranes. Advances in neural information processing systems, v. 12, 1999.

[105] Izhikevich, E. M. Dynamical systems in neuroscience. MIT press, 2007.

[106] Marder, E. Neuromodulation of neuronal circuits: back to the future. Neuron, v. 76, n. 1, p. 1-11, 2012.

[107] Lorenzen, F. et al. Quantum system under the actions of two counteracting baths: A model for the attenuation-amplification interplay. Physical Review A—Atomic, Molecular, and Optical Physics, v. 80, n. 6, p. 062103, 2009.